USING ARTIFICIAL TEXTURE TO ASSIST 3D RECONSTRUCTION

Wan-Ting Chen[1], Jen-Jer Jaw[2]
[1,2]National Taiwan University (NTU), No. 1, Sec. 4, Roosevelt Rd., Taipei 10617, Taiwan (R.O.C.),
Email: {r04521120@ntu.edu.tw[1], jejaw@ntu.edu.tw[2]}

KEY WORDS: Artificial texture, Stereo matching, Tie texture, 3D reconstruction

ABSTRACT: Stereo matching can effectively produce dense point cloud, but it may encounter great challenge when faced with low-textured image content. Even added with artificial texture, the location of the targeted scene, operation condition, and hardware requirement, among others, still demand considerable concerns to arrange for appropriate work scheme. Depending on the scene geometry, dimension and required degree of integrity, ways of texture projection and image acquisition may vary from one case to the other. The texture design aimed at this study contains two parts, one for scene or objects and the other for tie texture for consecutive image sections.

This work is currently at its early development and only employs digital cameras and video projectors. And dense matching software SURE was used to generate 3D point clouds. For projecting textures, we focus on analyzing and designing suitable textures taking the surface, geometry, and making succession of scene into consideration. On the other hand, the fine placements of projectors and camera stations are also crucial to maintaining quality imaging geometry. This study establishes appropriate work steps and rules by tackling afore-mentioned difficulties through simple sets of scene. And the applications to the engineering 3D reconstruction, survey, and monitoring will be soon followed.

1. INTRODUCTION

Stereo matching can effectively produce dense point cloud, but it may encounter great challenge. Photometric distortions and noise, specular surfaces, foreshortening, perspective distortions, repetitive pattern, transparent objects, occlusions and discontinuities, and uniform/ambiguous regions , as clearly indicated in Mattoccia (2012). Most of the challenges have their corresponding implementation modalities, and gradually attain improvement in the results of 3D reconstruction tasks. However, for three-dimensional reconstruction of the low texture regions, facilities for the conditions and needs of effectively setting up artificial texture still call for much improvement.

This study focus on using artificial textures to assist the 3D reconstruction for uniform scene or objects. Artificial textures and projectors configuration were designed and tested. Textures are divided into two parts. Artificial texture is for increasing the scene or object texture richness while tie texture for connecting adjacent stereo models to complete scene coverage. The way of giving artificial texture and configuring tie texture characterizes the significance of this study.

2. RELATED WORK

In computer vision patterns projected by projector is called structured light. Structured light scan system has at least a camera and a projector (Figure 2), and amid to measure shape of object. The principle is to project a strip consisting of light on object surface. Due to the surface variation, as seen in Figure 1, the projected light is not a straight line, which provides the geometric information to reconstruct 3D model.

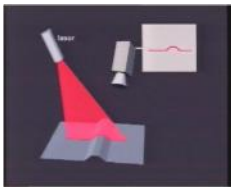

Figure 1 structured light system

Figure 2. video projector

Structured light can be used in many applications The ground truth of Muddlebury images often used in verifying the stereo matching performance utilized back and white structured light (Figure 3 & Figure 4). And it follows by assigning every pixel a unique code, then matching pair images and computing high accuracy disparity as the ground truth. Alexander et al. (2009) used color stripe structured light and different light condition to establish human face model (Figure 5 & Figure 6).

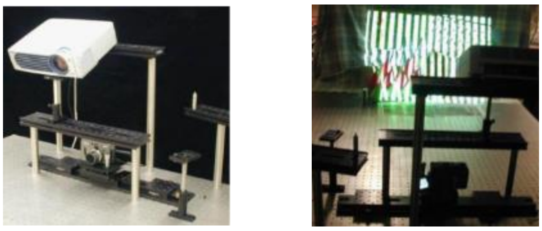

Figure 3. equipment (Scharstein and Szeliski, 2003)

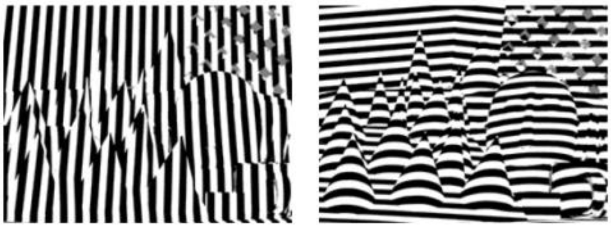

Figure 4. thresholded Gray-code images (Scharstein and Szeliski, 2003)

Figure 5. 15 images in different light condition (Alexander et al., 2009)

Figure 6. 3D model for human face (Alexander et al., 2010)

There are many forms of structure light, and can be derived into five categories (Van der Jeught & Dirckx, 2016, Figure 7) including color encoded projection, greyscale indexing, Fourier-based, sequential projections, and hybrid methods. Except the traditional fixed geometric patterns, Lin et al. (2016) combine two different geometry patterns with 4 colors to produce structured light by pseudorandom array for increasing the pattern variability (Figure 8).

The above mentioned method which used structured light have some common condition. They needed to calibrate the projector and structured light and coded the light. Then used the unique code to match left and right image. The most of the equipment only had on projector. The scene and object were small. Our research tried to use uncalibrated consumer video projector, and just used the richness of texture to compute the disparity of stereo pairs. In order to apply in the scene which over the projecting scope, we added the tie texture.

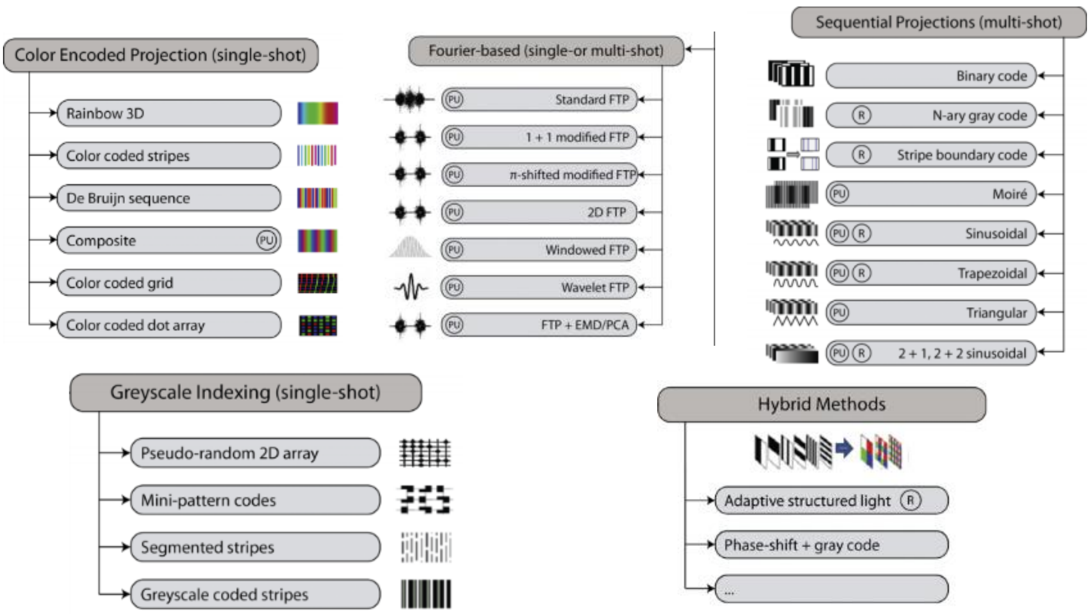

Figure 7. types of structured light (Van der Jeught & Dirckx, 2016)

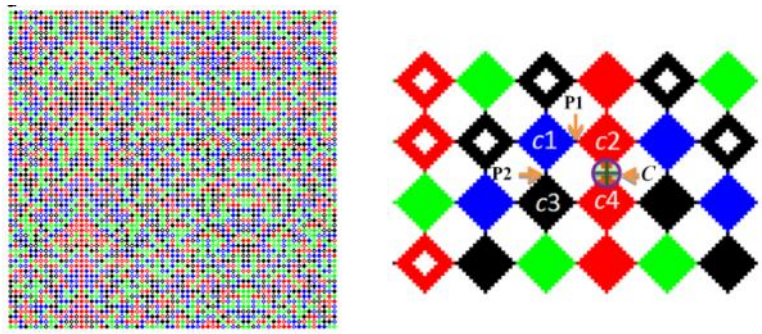

Figure 8. pseudorandom array (Lin et al., 2016)

3. METHODOLOGY

This work is now in the initial stage and currently focuses on the analysis and design of applicable textures that help in image matching and effectively connecting adjacent image pairs for a complete scene reconstruction. The detail is given as follows.

3.1 Pattern Design

The EPSON EP-1860 projector with standard resolution of 1024×768 is employed. In order to cooperate with the resolution of projectors, the size of textured images is also 1024×768.

3.1.1 Artificial texture

The element of artificial texture is square. We make 6 size of element including side length of 1, 2, 4, 8, 16, and 32.(Figure 9) The element size bigger means the density lower. The element has five colors: red, green, blue, black, and white, and the colors are random. Figure 10 showed 6 texture images.

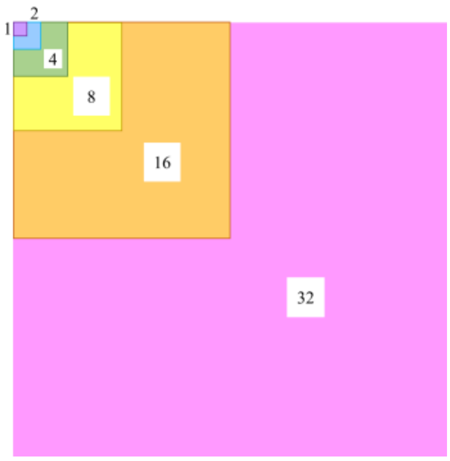

Figure 9 element size: side length 1, 2, 4, 8, 16, and 32

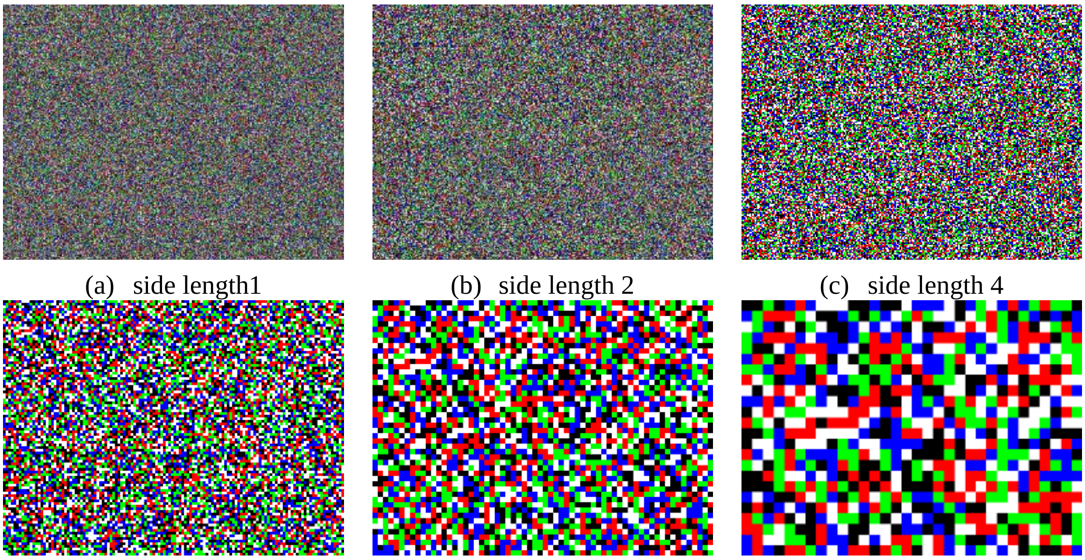

(a) side length1 (b) side length 2 (c) side length 4

(d) side length 8 (e) side length 16 (f) side length 32

Figure 10. artificial texture

3.2 Tie texture

Tie points have four colors: red, green, blue and black (Table 1) and combine with three different geometry types (Table 2). Figure 11 shows a 1024×768 image with 12 types of tie points.

Table 1. Tie point color.

Red	Green	Blue	Black

Table 2. Tie point type

Type 1	Type 2	Type 3

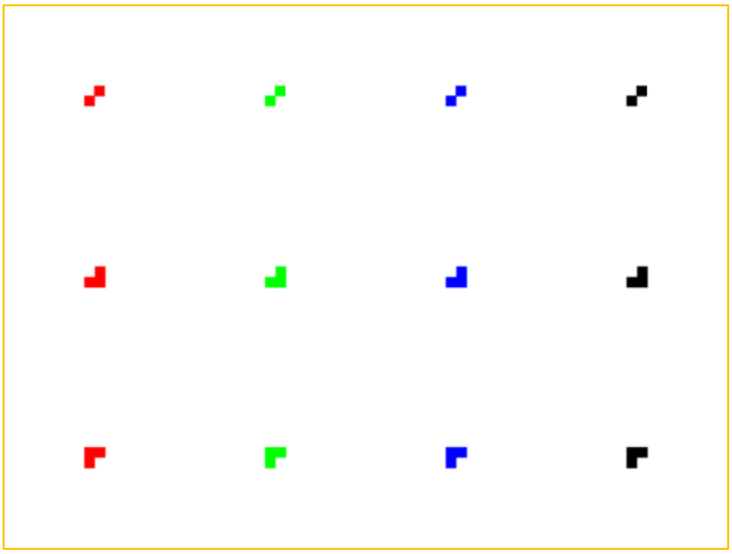

Figure 11. Patterns of tie point

3.3 Work planning

3.3.1 object distance

The requirement of the result is the accuracy of object direction (σ_D) and ground sampling distance (GSD) are ≤1 mm and the image overlap is at least 80%. According the principle of disparity can derive suitable distance D with the camera parameters and matching method.

$$D = \sqrt{fB\frac{\sigma_D}{\sigma_p}} \quad (1)$$

3.3.2 Projectors configuration

Figure 12 showed the projectors configuration, location B projects tie texture. A projects the artificial texture at first. After acquiring image pairs, the projector is put on C and acquire image pairs again.

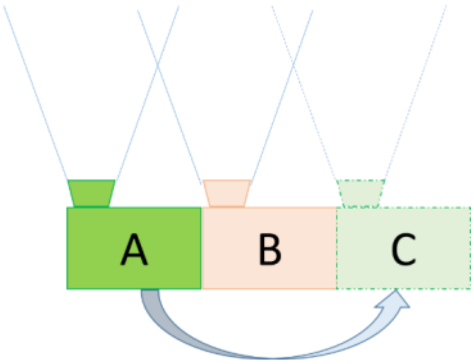

Figure 12 configuration of projectors

3.4 Work flow

Artificial texture and tie texture are projected separately. Experimental images are shot at three sites, and each site gets image pairs of artificial texture and tie texture. Among them, image pairs of artificial texture are including six different density textures. The matching software is SURE. Then, the outcomes are of different density analyzed and tie texture is used to connect pairs of distinct sites. (Figure 13)

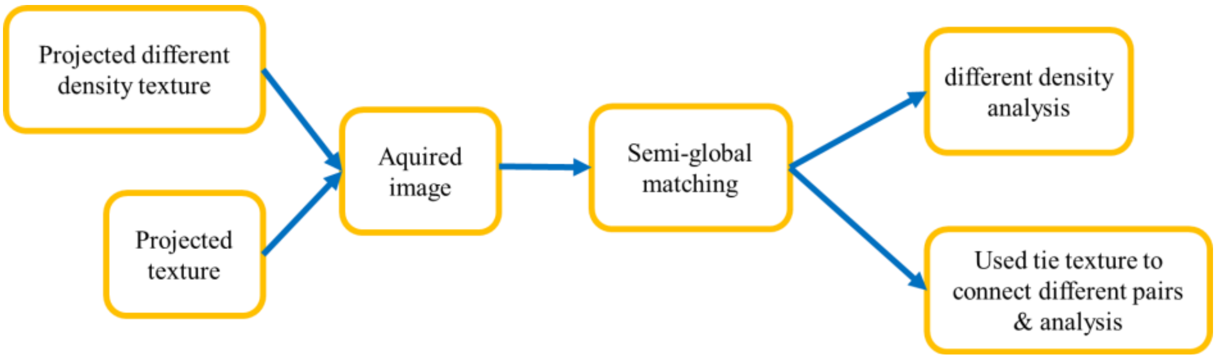

Figure 13 work flow

4.4 RESULTS AND ANALYSIS

As mentioned above, Table 3 showed work planning of experiment.

Table 3. work planning

Camera	Canon 760D
image size	3984×2656 pixel
pixel size	0.0056 mm
accuracy of object direction σ_D	0.9 mm
disparity accuracy (pixel) σ_p	0.31
ground sampling distance (GSD)	0.6 mm
base length B	0.359 m
principle distance f	35 mm
object distance D	2.55 m

4.1 Texture density

Six different density artificial texture images were used. Every texture image shot one pair of experimental image, so totally acquired 12 images (Figure 14). The result displayed that the density of texture decrease for side length 1 to 4, but the number of points increase. Relatively, the number of points dropped sharply for side length 8 to 32. (Table 4 & Figure 16)

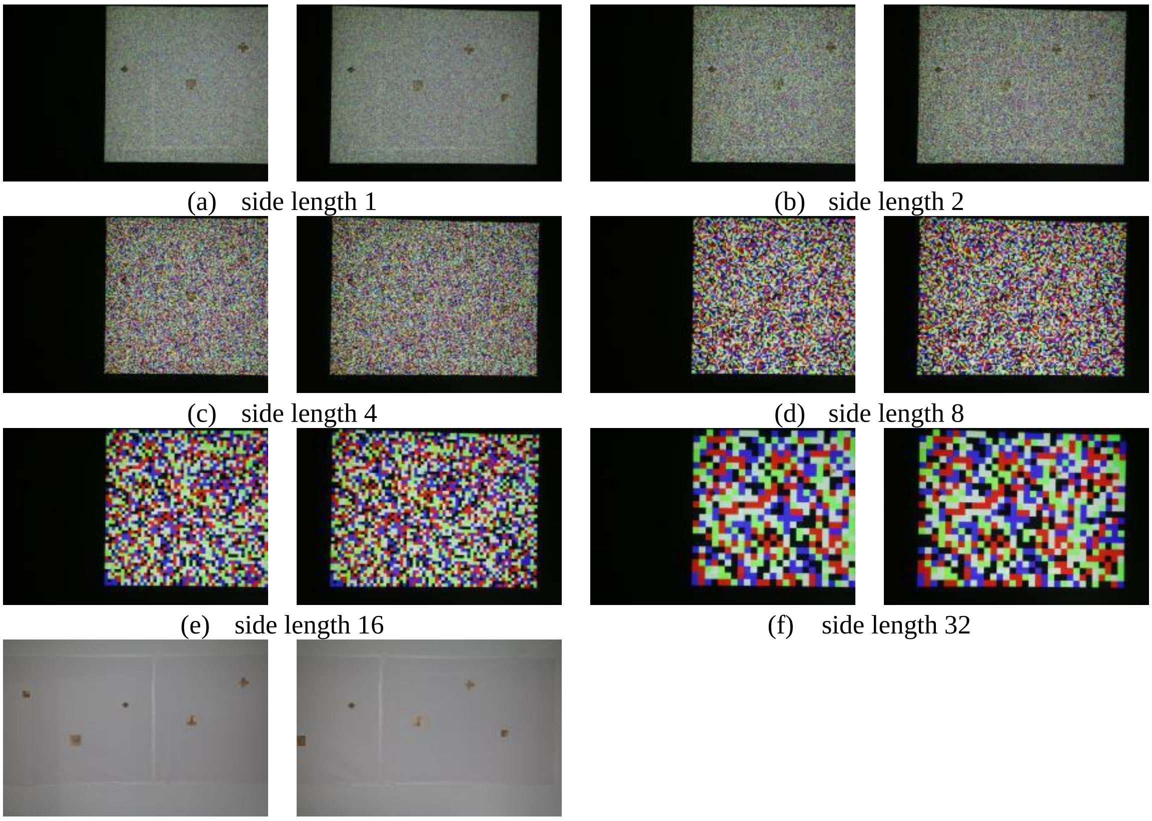

(a) side length 1

(b) side length 2

(c) side length 4

(d) side length 8

(e) side length 16

(f) side length 32

(g) untextured

Figure 14. images

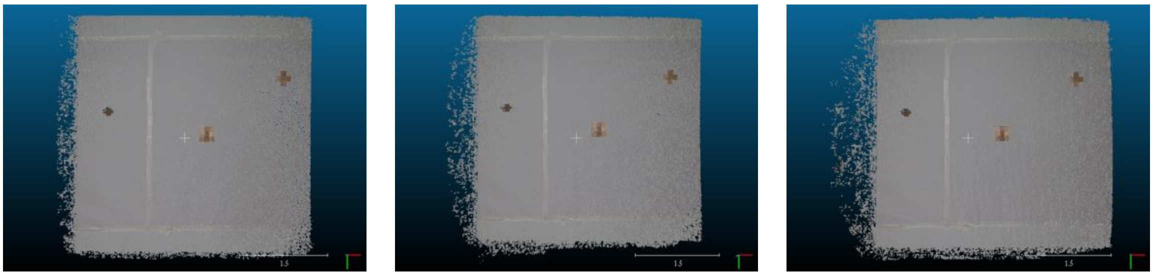

(a) side length 1 (b) side length 2 (c) side length 4

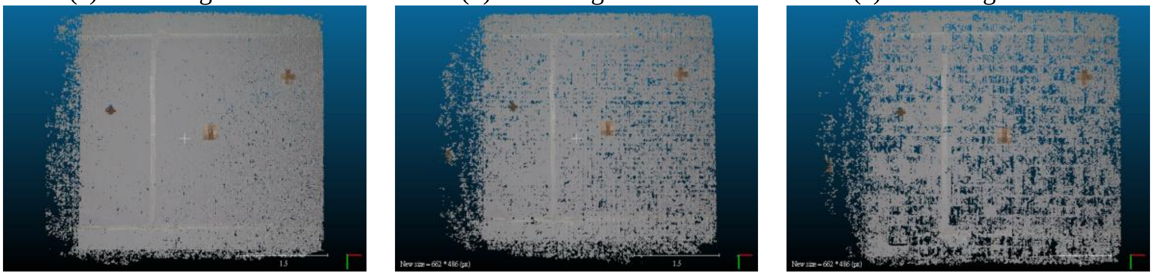

(d) side length 8 (e) side length 16 (f) side length 32

Figure 15. 3D reconstruction

Table 4. number of points

side length 1	10,753,721
side length 2	11,230,430
side length 4	11,459,923
side length 8	8,968,481
side length 16	6,057,061
side length 32	3,825,465

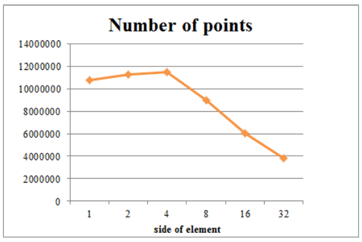

Figure 16. number of points

4.2 Tying different texture pairs

At three locations which were 35.856 cm between neighboring ones, got two groups of different artificial texture images and tie texture images. Figure 17 and Figure 18 showed the acquired images. There were 6 tie points between group 1 and group 2, and we used these points to proceed coordinate conversion to connect two groups into one group (Figure 19 & Figure 20 & Figure 21). For verifying outcomes, we set 4 control points (Table 5), and the model was transformed to object space. Then we checked the side length of wood feature and other feature point. The maximum difference between object space and point cloud was 0.0005 m. It corresponded accuracy of object direction in work planning.

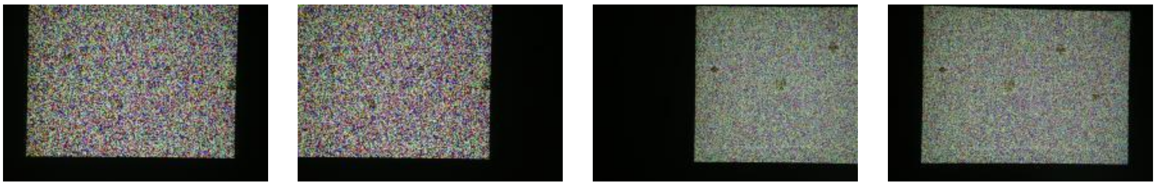

(a) Group 1 (b) Group 2

Figure 17. experimental images, artificial texture

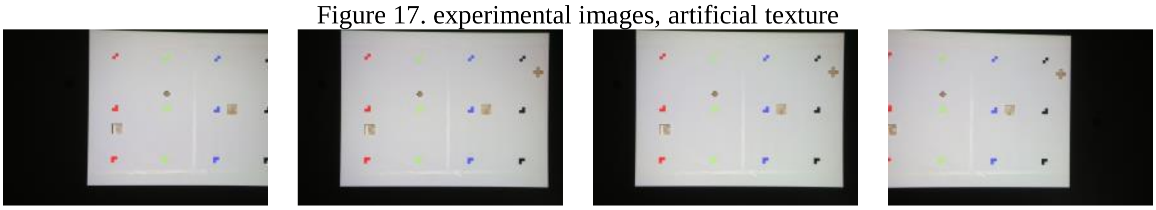

(a) Group 1 (b) Group 2

Figure 18. experimental images, tie texture

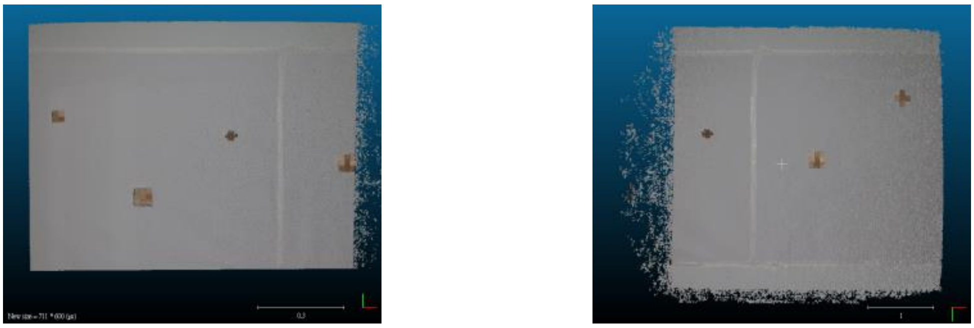

Figure 19 point cloud, untextured

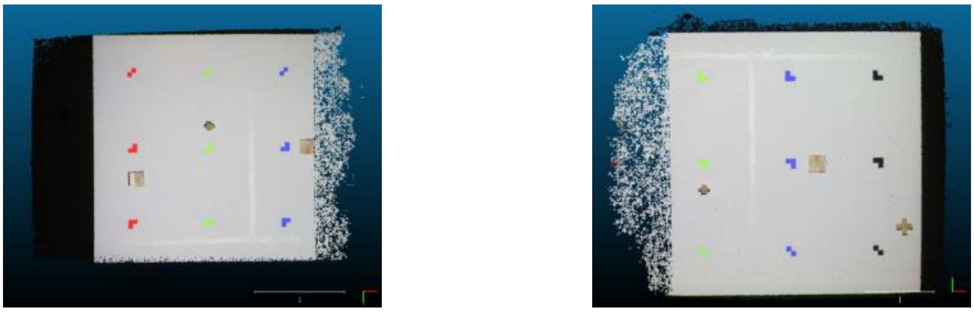

(a) Group 1 (b) Group 2

Figure 20. point cloud, tie texture

Figure 21. point cloud connection

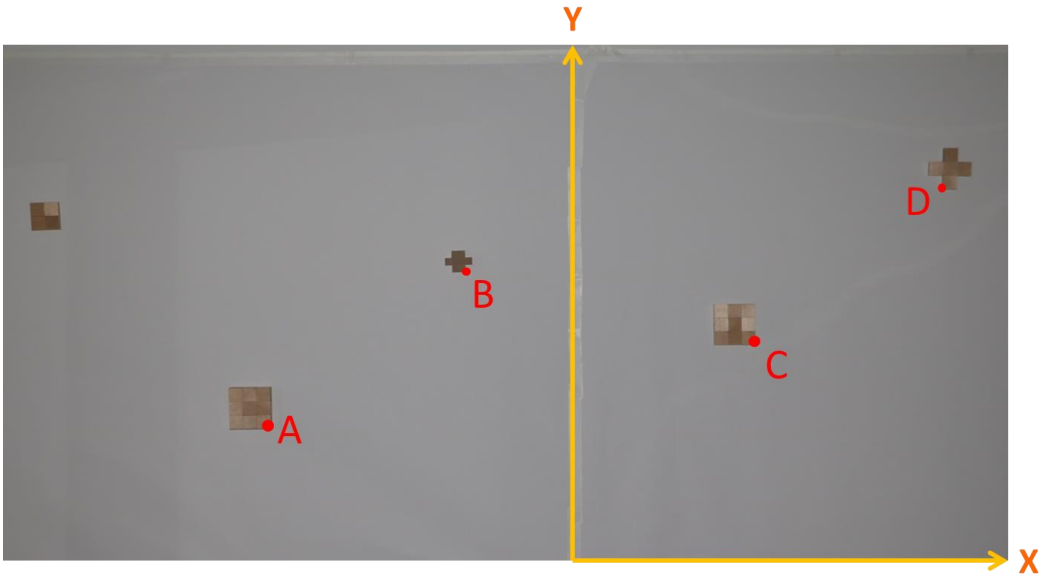

Figure 22 control points

Table 5 control points

ID	X (m)	Y (m)	Z (m)
A	-0.4360	0.2400	0.0207
B	-0.1495	0.4665	0.0198
C	0.2795	0.3555	0.0105
D	0.5550	0.5855	0.0104

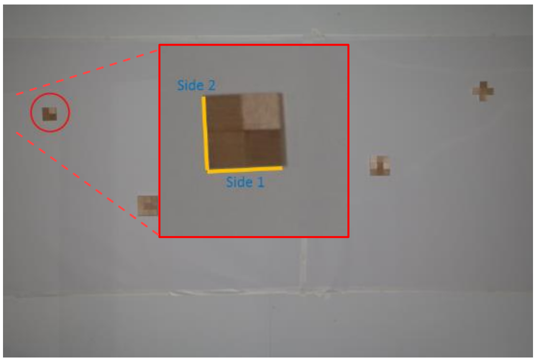

Figure 23 check 1

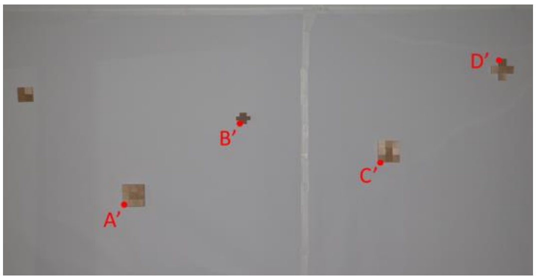

Figure 24 check 2

Table 6 check 1 (m)

ID	Measured	Point cloud	Difference
side 1	0.0402	0.0399	0.0003
side 2	0.0402	0.0403	0.0001
height	0.0104	0.0108	0.0004

Table 7 check2

ID	Measured			Point cloud			Difference		
	X (m)	Y (m)	Z (m)	X (m)	Y (m)	Z (m)	X (m)	Y (m)	Z (m)
A’	-0.4965	0.2400	0.0210	-0.4968	0.2400	0.0213	-0.0003	0.0000	0.0003
B’	-0.1697	0.4665	0.0196	-0.1696	0.4668	0.0193	0.0001	0.0003	-0.0003
C’	0.2189	0.3555	0.0108	0.2185	0.3559	0.0105	-0.0004	0.0004	-0.0003
D’	0.5550	0.6456	0.0104	0.5548	0.6451	0.0099	-0.0002	-0.0005	-0.0005

5. CONCLUSION AND FUTURE WORK

The result of density experiment showed that the texture density affected the integrity of 3D reconstruction. For different scene, the suitable texture was also not the same. The outcomes of experiment 2 verified that using tie texture and effective projectors configuration could increase the scope of reconstruction. At present stage of work, experiment 2 used coordinate conversion by connecting points. We will compute connecting relative orientation by connecting points in next step. In addition, to improve the work efficiency, the density of texture will be evaluated by the characteristic of scene and be as one work of scheme.

References

Alexander, O., M. Rogers, W. Lambeth, M. Chiang, and P. Debevec, P., 2009. Creating a photoreal digital actor: The digital emily project. InVisual Media Production, IEEE Conf. on CVMP'09, pp. 176-187.

Alexander, O., M. Rogers, W. Lambeth, J. Y. Chiang, W. C. Ma, C. C. Wang, and P. Debevec, 2010. The digital emily project: Achieving a photorealistic digital actor, Computer Graphics and Applications, IEEE,30(4), 20-31.

Gerig, G., 2012. Structured lighting, 3D Computer Vision, URL: http://www.sci.utah.edu/~gerig/CS6320-S2013/Materials/CS6320-CV-S2012-StructuredLight.pdf.

Hirschmüller, H., 2008. Stereo Processing by Semiglobal Matching and Mutual Information, IEEE Transactions on Pattern Analysis and Machine Intelligence, 30(2):328-3341.

Kraus, K., 2007. Photogrammetry, Geometry from Images and Laser Scans. de Gruyter, Berlin, 2nd edition edition. 459p.

Lin, H., L. Nie, and Z. Song, 2016. A single-shot structured light means by encoding both color and geometrical features, Pattern Recognition, 54:178-189.

Mattoccia, S., 2012. Stereo Vision: Algorithms and Application , University of Bologna, URL:
http://vision.deis.unibo.it/~smatt/Seminars/StereoVision.pdf (last date accessed: 123 April 2016)

Ma, W. C., 2008. A framework for capture and synthesis of high resolution facial geometry and performance, Ph.D. Dissertation, National Taiwan University, Taipei, 121 p.

Scharstein, D., and R. Szeliski, 2003. High-accuracy stereo depth maps using structured light. IEEE Computer Society Conference on Computer Vision and Pattern Recognition (CVPR 2003), 1:195-202.

Salvi, J., J. Pagès, and J. Batlle, 2004. Pattern codification strategies in structured light systems, Pattern recognition, 37(4):827-849.

Siebert J. P., and S. J. Marshall, 2000. Human body 3D imaging by speckle texture projection photogrammetry, Sensor Review, 20(3):218-226.

Van der Jeught, S., and J. J. Dirckx, 2016. Real-time structured light profilometry: a review, Optics and Lasers in Engineering, http://dx.doi.org/10.1016/j.optlaseng.2016.01.011i

Wenzel, K., M. Abdel-Wahab, A. Cefalu, and D. Fritsch, 2011. A Multi-Camera System for Efficient Point Cloud Recording in Close Range Applications. Low Cost 3D (LC3D) workshop, Berlin.